Supplemental Material: Light mediated cascaded locking of multiple nano-optomechanical oscillators

E. Gil-Santos,[1] M. Labousse,[1] C. Baker,[1] A. Goetschy,[1,2] W. Hease,[1,2] C. Gomez,[3] A. Lemaître,[3] G. Leo,[1] C. Ciuti,[1] and I. Favero[1]

[1]*Matériaux et Phénomènes Quantiques, Université Paris Diderot, CNRS UMR 7162, Sorbonne Paris Cité, Paris, France*
[2]*Institut Langevin, ESPCI Paristech, CNRS UMR 7587, PSL Research University, 1 rue Jussieu, 75005, Paris, France*
[3]*Centre de Nanosciences et de Nanotechnologies, CNRS, Université Paris Sud, Université Paris-Saclay, C2N-Marcoussis, 91460 Marcoussis, France*

(Dated: January 4, 2017)

CONTENTS

Fabrication 2

Experimental setup 2

Numerical computation 4

Thermo-optical effects and optical disorder 4

References 7

FABRICATION

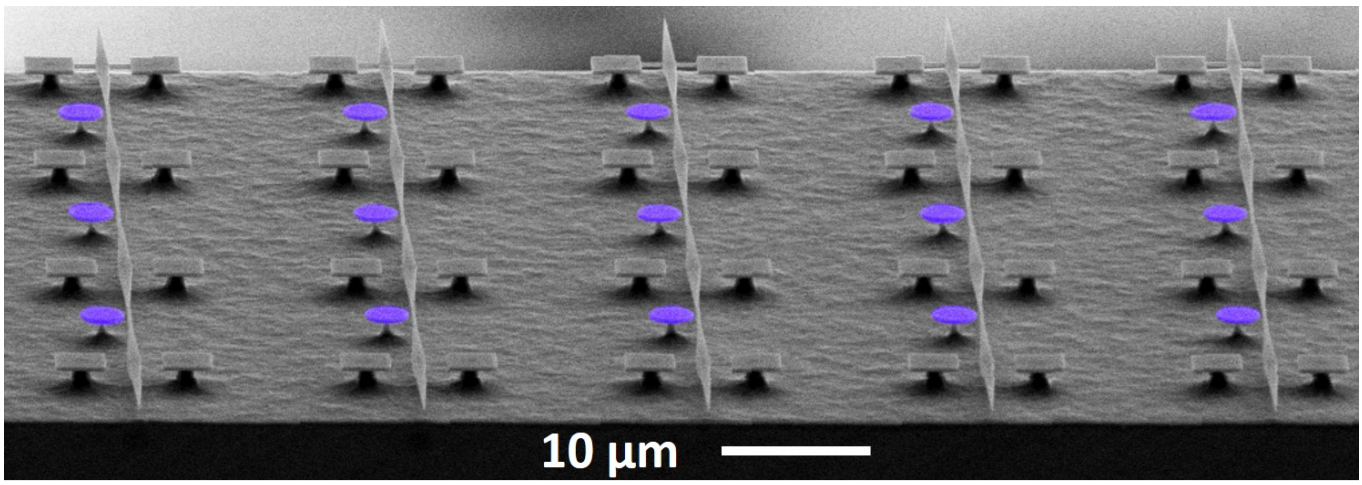

Figure 1. Scanning electron microscope image of five cascaded devices. Each one contains three optomechanical disk resonators with identical size: 1.5 μm in radius and 320 nm thick.

Arrays of miniature disk resonators and waveguides are fabricated out of a GaAs (320 nm)/$Al_{0.8}Ga_{0.2}As$ (2,000 nm)/GaAs wafer, grown by molecular beam epitaxy. The disks are 320 nm thick, while their radius is of 1.5 μm. GaAs disks sit on AlGaAs pedestals, whose height is about 2 μm and radius is smaller than 150 nm. The disks are positioned in the vicinity of GaAs tapered suspended waveguides to allow evanescent optical coupling [See Fig.S1]. Disks and waveguides are patterned in a resist mask by electron-beam lithography and dry etched by inductively coupled plasma reactive ion etching with a mixture of SiCl4 and Ar plasmas. The AlGaAs sacrificial layer is selectively under-etched by HF to form the pedestals. A diluted HF:H_2O solution (1.22% in volume) at 4°C is combined with a slow agitation in the solution to reach a pedestal of radius below 150 nm. A typical chip is 1 mm wide, 3 mm long and contains hundreds of waveguides separated by a distance of 20 μm. On the same chip, we include waveguides that address one, two and three disks. Each disk is placed far away from its neighbors ($\simeq$25 microns) to avoid direct coupling between their mechanical or optical modes. A mesa structure of height 150 μm is fabricated to allow the access of microlensed fibers, which inject and collect the light to the integrated waveguides, as depicted in Fig. S2.

EXPERIMENTAL SETUP

The experimental set-up is depicted in Fig. S3. Monochromatic light from an external tunable cavity diode laser is fiber-guided, polarization-controlled, injected into and collected from the integrated waveguides using microlensed fibers. Importantly, the waveguide input/output ports consist in inverted tapers that allow adiabatically injecting and collecting light. The tapers are specifically designed to suppress back-reflections and Fabry-Perot interferences, and increase the optical coupling efficiency to 50% for TM modes. In absence of back-reflection, the propagation of light is unidirectional. Both the microlensed fibers and the sample are placed on top of XYZ micro-positioning stages, in order to align of the fibers and waveguides with

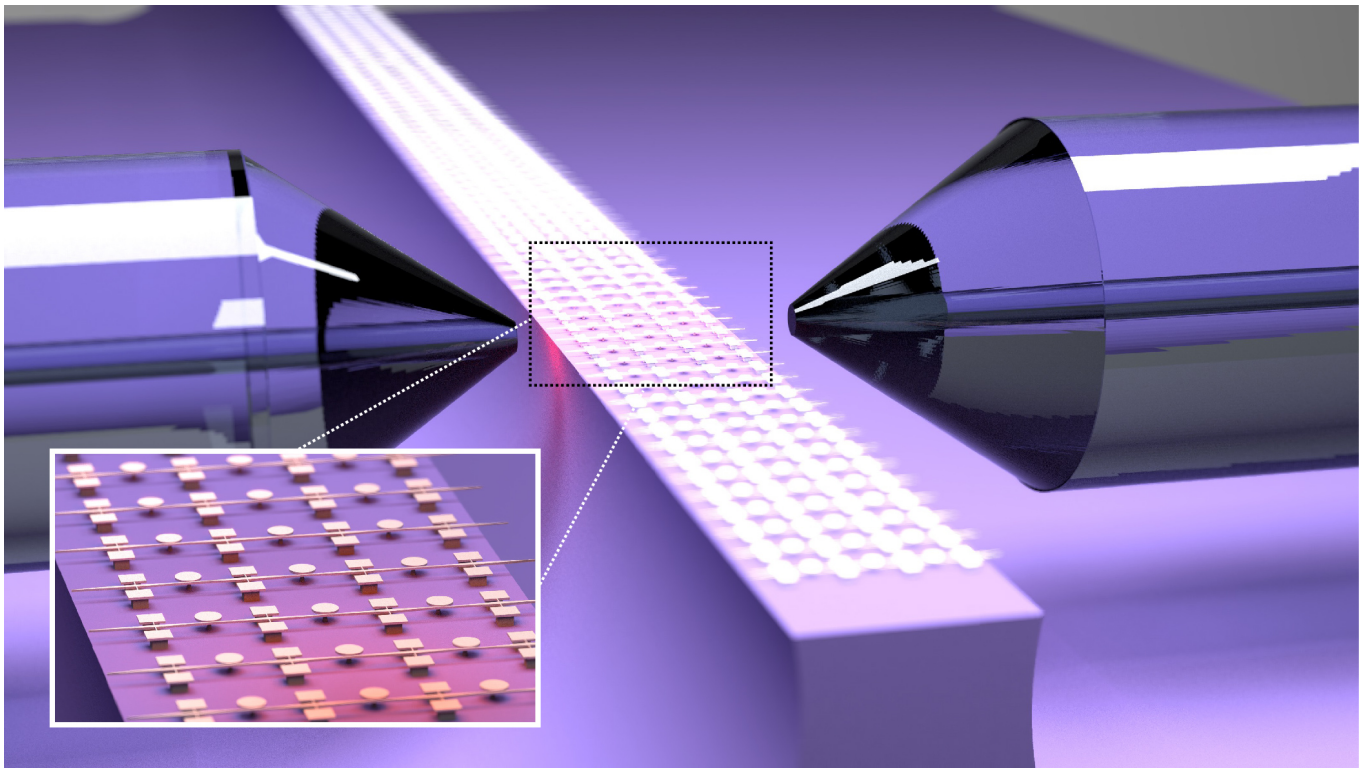

Figure 2. Mesa structure. The resonators and their suspended coupling waveguide are elevated above the chip on a mesa/ridge-like structure (center) in order to enable lensed fiber access for both light injection and collection. The 125 micron diameter lensed fibers and the resonator arrays are represented here to scale.

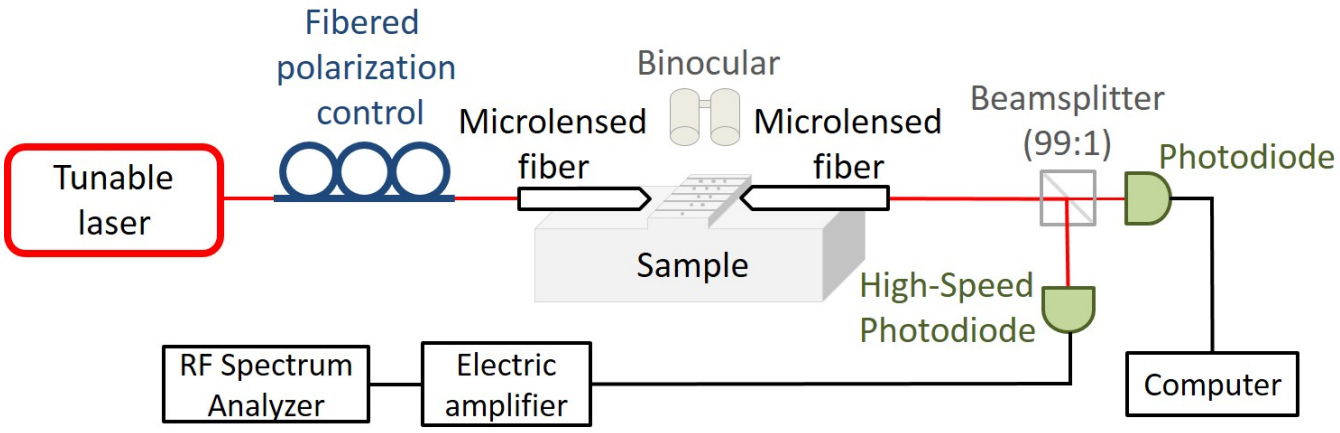

Figure 3. Experimental setup. The system allows to obtain at the same time mechanical and optical information.

the help of a binocular microscope atop of them. The collected optical signal is split in two, in order to analyze in parallel the DC and AC components bearing the optical and the mechanical information. 99 % of the collected power is injected into a fast photodiode, whose output electrical signal is amplified and sent onto a spectrum analyzer that extracts the mechanical information. The remaining 1 % of power is sent onto a switchable gain photodiode connected to a computer in order to track the time-averaged optical signal.

NUMERICAL COMPUTATION

We solve Eq. (1) numerically with a first order integration using MATLAB2014. We prescribe the thermal number of phonons as

$$n_{\mathrm{th}} = \frac{1}{\exp\left(\frac{\hbar\Omega}{k_B T}\right) - 1} \tag{1}$$

with k_B being the Boltzmann constant and $T = 300$ K, the ambient temperature. The final simulation time is $\Omega t_f = 10^5$ with a time step of $\Omega\Delta t = 2\times 10^{-4}$ and a recording of $(\alpha_k(t), \beta_k(t))$ every 500 time steps. We then compute the output optical intensity from which we compute the noise power spectral density with the Welch method implemented in MATLAB2014.

THERMO-OPTICAL EFFECTS AND OPTICAL DISORDER

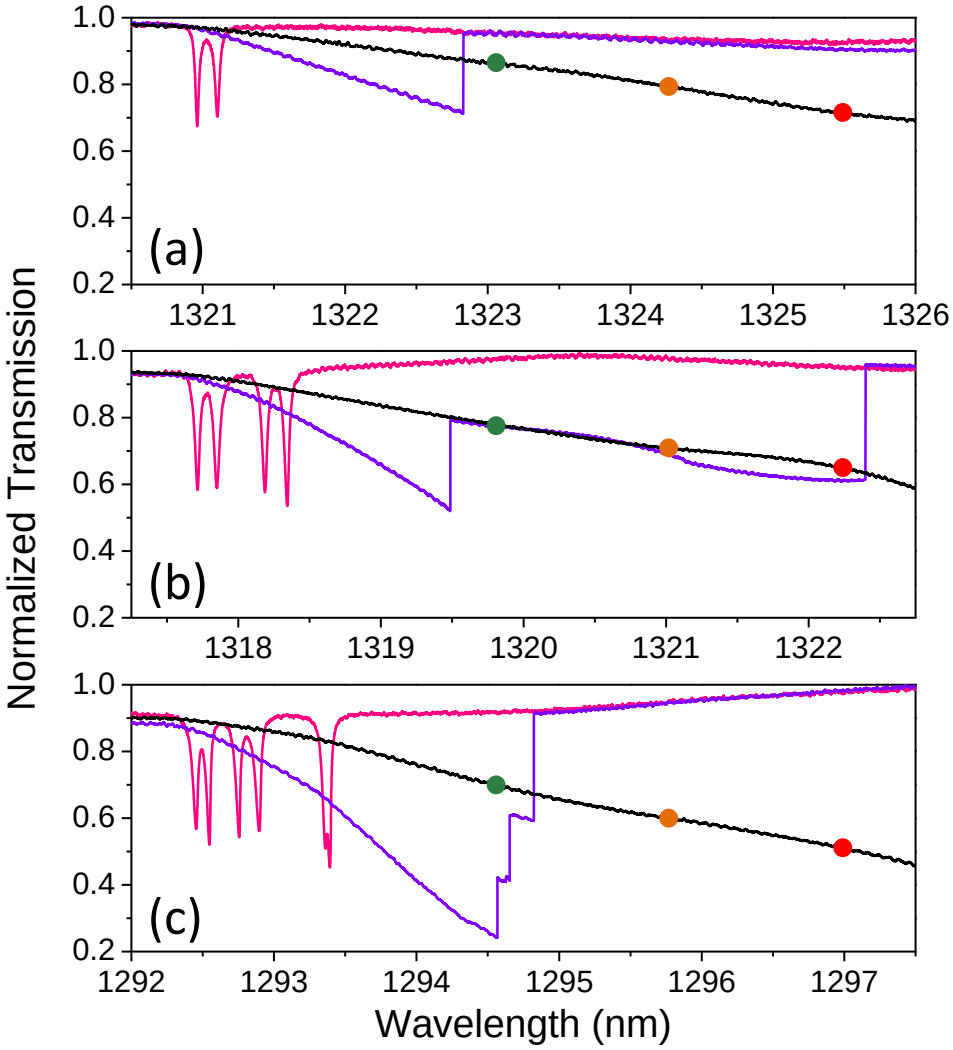

Figure 4. Normalized optical spectra: (a) a single disk, (b) two disks and (c) three disks, with power levels in the waveguide of 1 μW (pink), 0.35 mW (violet) and 1 mW (black). The spectra correspond to the same devices measured in Figs 2 and 3 of the main text. Those mechanical spectra has been obtained by injecting 1 mW in the waveguides. A red spot indicates the maximum optical wavelength used on those experiments, corresponding to the red spectra shown in Fig. 2 of the main text.

GaAs disk resonators present some level of residual optical absorption at the surface. The amplitude of surface absorption varies from one semiconductor material to another, and also depends on specific surface treatments. In the low optical power limit, surface absorption does not impact experimental results, but at large power and with the high optical Qs at play, it results in a local heating with optical and mechanical consequences. Figure S4(a) shows optical spectra acquired on a single disk for different optical powers injected into the waveguide. At low power, the spectrum displays a doublet structure originating from the hybridation of clockwise and counter-clockwise modes. Both resonances have a symmetric Lorentzian shape, and their intrinsic optical Q is about 10^5. As the power is increased, we observe a distortion of the optical resonance, which is a signature of heating of the disk. The thermal distortion of optical resonances in GaAs disks is known to result from the thermo-optic effect, with little role played by thermal expansion of the disk. The temperature increase ΔT corresponding to an optical resonance shift $\Delta\lambda$ is $\Delta T = n\frac{\Delta\lambda/\lambda}{dn/dT}$. At the largest optical power used in our experiments, the wavelength shift is of 5 nm, which corresponds to $\Delta T \simeq 60$ K. In our experiments, we avoid wavelength shifting by more than 5 nm to avoid thermal damage. As the mechanical properties of GaAs change with temperature, heating also leads to changes in the measured mechanical resonance frequency. A temperature increase reduces the Young modulus of GaAs, making the disk "softer" and lowering its mechanical resonance frequency, as shown in Fig. 2 of the main text.

The same thermal optical distortion is observed in configurations containing multiple optomechanical disks along the same waveguide. Figures S4(b) and (c) show the optical spectra acquired on devices consisting on two and three disks respectively, as a function of the optical power injected on the waveguide. At low power, the spectra show two and three doublets corresponding hybrid clockwise/counter-clockwise modes of each disk. Again, Lorentzian shapes of the optical resonances indicate no heating; and the intrinsic optical quality factor Q_s are about 10^5. Doublets are distanced by about 400 pm, corresponding to an initial optical disorder of 3×10^{-4}. As the power is increased, thermal distortion produces merging of the optical resonances. At the highest power used in experiments, the optical wavelength shift produced by thermal distortion is larger than the initial optical disorder, which permits simultaneous injection of laser light in all the disks. We estimate that the effective optical disorder in such configuration is below 10^{-5}. The devices shown here are those of Figures 2 and 3 of the main text, and mechanical spectra have been acquired with 1 mW of optical power in the waveguides. The largest optical wavelengths used in these experiments, which correspond to the red spectra shown in Fig. 2 of the main text, are indicated by red spots in Fig. S4(a)-(c).

In order to quantitatively describe such situations, a formalism combining the electromagnetic coupled mode theory and a linear thermo-optic coupling can be employed. The resonance wavelength λ_0 of resonator i, $\lambda_{0,i}$, is linked to the resonator's temperature T_i through the following equation [1, 2]:

$$\lambda_{0,i}(T_i) = \lambda_{0,i}(T_0) + \frac{d\lambda_{0,i}}{dT}\Delta T = \lambda_{0,i}(T_0)\left(1 + \frac{1}{n}\frac{dn}{dT}\Delta T\right) \tag{2}$$

where T_0 is the temperature of the environment (300 K), n the refractive index of bulk GaAs, $dn/dT = 2.3\times10^{-4}$ the thermo-optic coefficient of GaAs and $\Delta T = T_i - T_0$. We next define for each resonator a normalized optical transmission function Λ_i [1]:

$$\Lambda_i(\lambda, T_i) = 1 - \frac{C_i}{1 + \left(\frac{\lambda - \lambda_{0,i}(T_i)}{\delta\lambda_i/2}\right)^2} \tag{3}$$

with C_i and $\delta\lambda_i$ the contrast and FWHM of the WGM resonance of resonator i. Finally we relate the change in temperature of each resonator to the amount of optical power it absorbs and its thermal anchoring to the environment [1]:

$$\frac{dT_i}{dt} = P_i A\frac{1-\Lambda_i(\lambda, T_i)}{mc} - \frac{G}{mc}(T_i - T_0) \tag{4}$$

Here A, m, c and G respectively denote the fraction of dissipated power lost as heat in the resonator, the resonator mass, resonator material heat capacity and the thermal conductance between the disk and substrate, see reference [1] for more details. P_i is the optical power reaching resonator i:

$$P_i = P_0\prod_{j<i}\Lambda_j \tag{5}$$

It is the laser power P_0 injected into the beginning of the waveguide times the product of the transmission functions of all upstream resonators. As we can see from Eq. 5, the order in which the resonators are arranged along the waveguide will

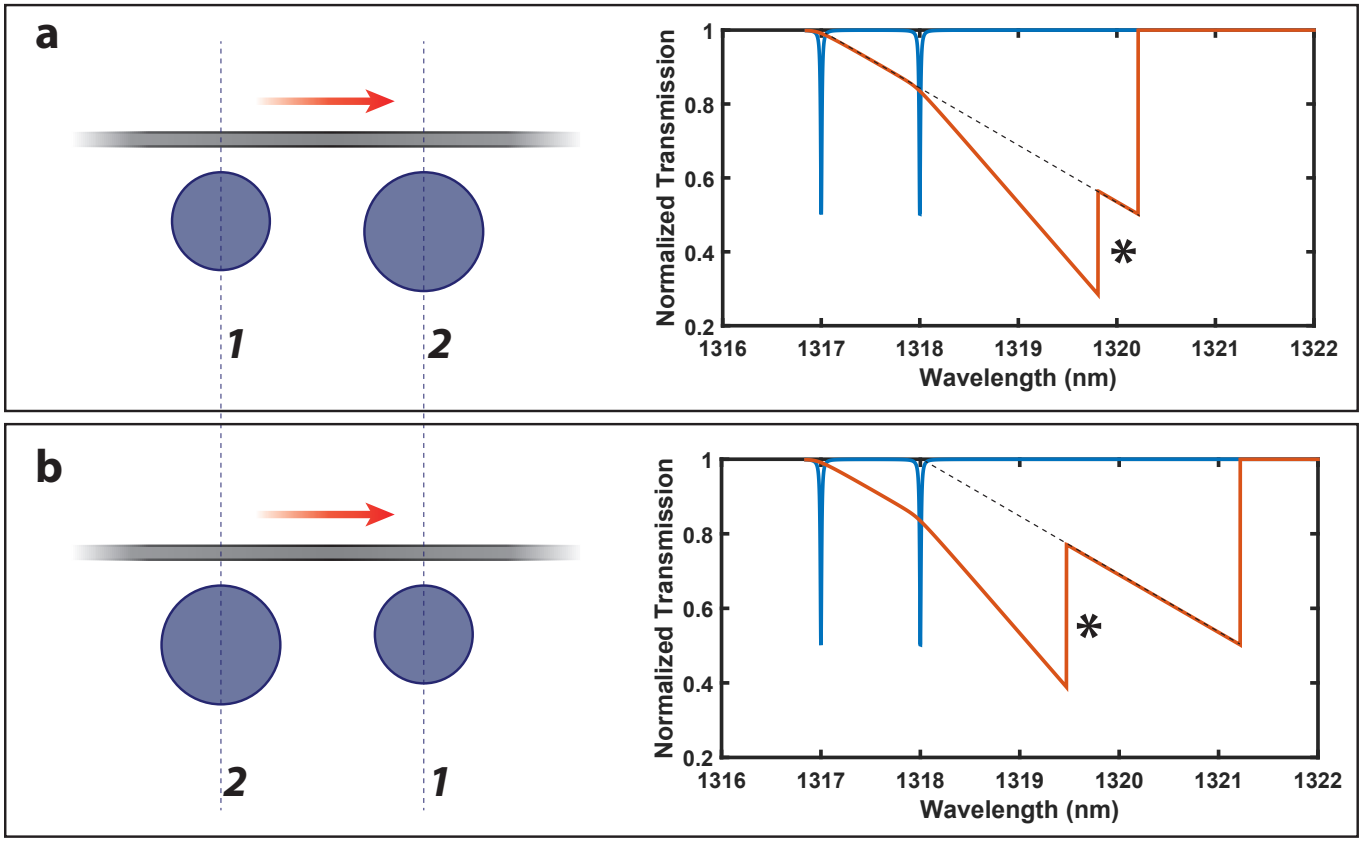

Figure 5. Influence of resonator order along the waveguide. (a) Left: the smallest resonator –**1**– is positioned first along the waveguide (red arrow is light propagation direction). Right: numerically calculated normalized transmission through the waveguide, for low (1 μW; blue) and high (0.35 mW; red) optical power. The asterisk * corresponds to a jump out of resonator **2**, at which point light is only coupled into resonator **1**, as can be seen by regressing the thermo-optic slope back to $\lambda_{0,1}(T_0)$ (dashed grey line). (b) Left: the largest resonator –**2**– is positioned first along the waveguide. Right: numerically calculated normalized transmission through the waveguide for identical powers. The asterisk * corresponds to a jump out of resonator **1**, at which point light is only coupled into resonator **2**, as can be seen by regressing the thermo-optic slope back to $\lambda_{0,2}(T_0)$ (dashed grey line).

influence how much optical power reaches each resonator, and must therefore be taken into account. This influence is shown in Fig. S5. Using the three coupled equations Eqs. (2), (3) and (4), we numerically calculate the normalized optical transmission through two cascaded resonators, at low and high laser power, as a function of the order of the resonators along the waveguide. (This is done with 2 nested loops, the outer over λ and the inner over time for the system to reach thermal equilibrium). While at low laser powers (blue) the order of the resonators along the waveguide has no influence, at higher powers the transmission curve appears fundamentally different. Interestingly, the pattern of thermo-optic jumps marked by an asterisk provides a unique fingerprint that allows us to unambiguously determine the order in which the resonators are aligned in our experimental data.

This is shown in Fig. S6(a), where we fit the normalized transmission through three cascaded resonators. The pattern of thermo-optic jumps in the medium and high power measurements allow us to determine the resonators are arranged in order of increasing size along the waveguide, with the smallest upstream and the largest downstream. In addition to determining the positioning of the resonators, this fit allows us to precisely determine the power coupled into each resonator, as shown in Fig. 6(b). As previously mentioned, while for low power, light is never simultaneously injected into all three resonators, at higher power the thermo-optic shift allows us to overcome the initial fabrication-induced optical disorder. This can be further quantified: the fitting procedure records the resonance wavelength $\lambda_{0,i}(T)$ of each resonator for each laser wavelength. The full evolution is shown in Fig. S7. In the high power plot of Fig. 6(b), at 1297 nm we have $\lambda_{0,3}(T) - \lambda_{0,1}(T) = 2$ pm, a four hundred fold reduction over $\lambda_{0,3}(T_0) - \lambda_{0,1}(T_0) = 800$ pm at low power.

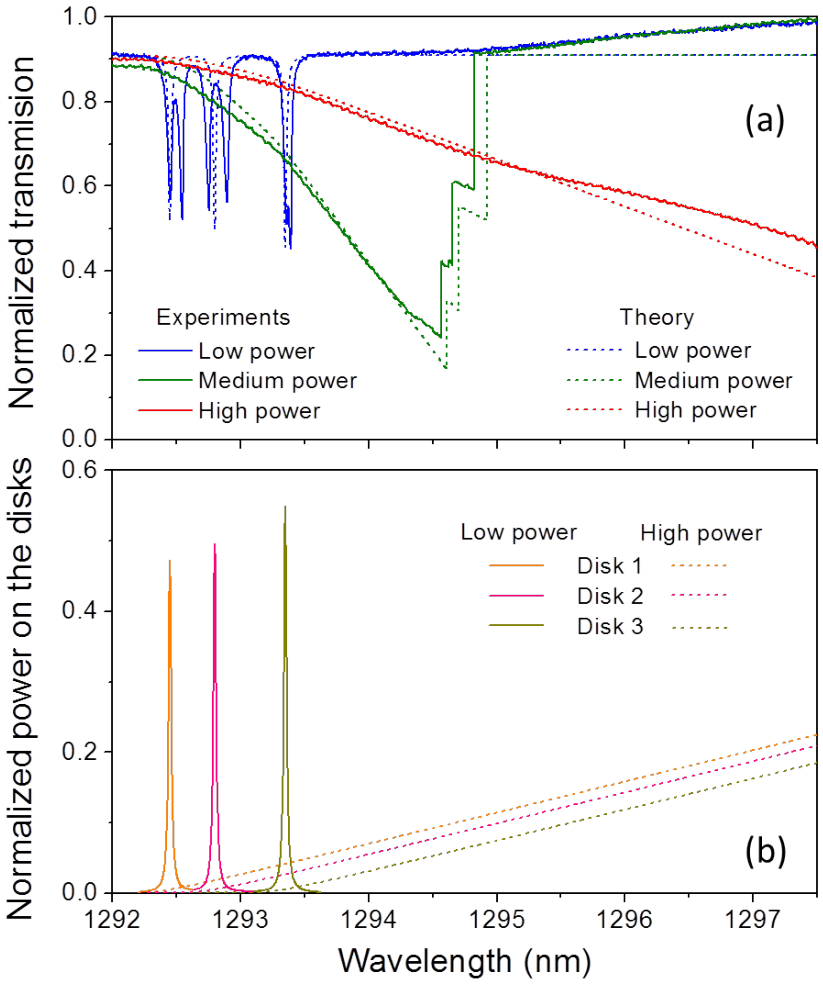

Figure 6. Fitting the normalized transmission through three cascaded resonators.(a) Experimental (solid lines) and theoretical transmission through three cascaded optical resonators, at low (blue ; 1 μW), medium (green; 0.35 mW) and high (red; 1 mW) optical powers. In the numerical fit each resonance is modeled as a singlet. (b) From the numerical fit, we extract for each laser wavelength the normalized power injected into each resonator.

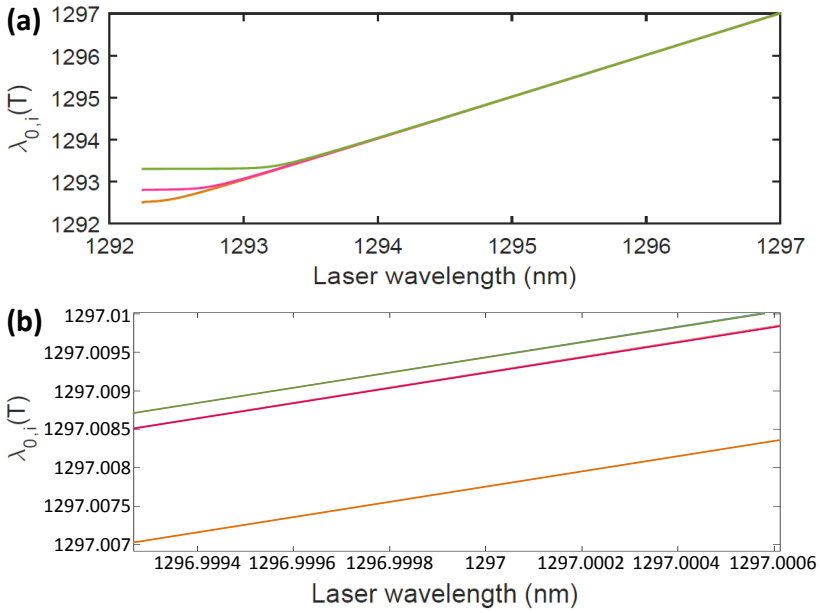

Figure 7. Evolution of the optical disorder in the three cascaded resonators.(a) Resonance wavelengths $\lambda_{0,i}(T)$ of the three resonators as a function of the laser wavelength. The spectral merging of the three resonances is made possible by the thermo-optical effects. (b) Spectrally zooming on three resonances in the thermo-optical regime, we directly observe a reduced optical disorder in the 10^{-6} range.

[1] Christophe Baker, Sebastian Stapfner, David Parrain, Sara Ducci, Giuseppe Leo, Eva M. Weig, and Ivan Favero. Optical instability and self-pulsing in silicon nitride whispering gallery resonators. *Optics Express*, 20(27):29076–29089, December 2012.

[2] Christopher Baker. *On-chip nano-optomechanical whispering gallery resonators*. PhD thesis, Université Paris Diderot, 2013.